Macromol. Symp. **2006**, 243, 247–260 DOI: 10.1002/masy.200651123

Formation of Nanostructures in Multi Component Systems Based on Organic Polymer and Coordination Metal Compound

Nataly Kozak, Yurij Nizelskii, Nadya Mnikh, Vladimir Shtompel, Oleg Grischuk*

Summary: Structuring of polyurethane (PU) networks is analyzed under influence of transition metal coordination compounds: mono-ionic β-diketonates and polyheteronuclear metal-organic complexes. Formed in situ nanostructures both organic and inorganic were found in organic polymer modified with coordination metal compound. Influence of coordination junction point spatial symmetry and content of metal ion in modifier on structure and dielectric characteristics of modified PUs is analyzed using X-ray, EPR, SEM and transmission optical microscopy, DRS and DSC methods.

Keywords: dielectric properties; EPR; nanoheterogeneity; polyurethane networks; transition metal coordination complex; X-ray analysis

Introduction

Formation of a polymer matrix in the presence of coordination metal compounds favors creation of a new hierarchy in structural organization of the polymer as compared with metal free system. This effect is caused by complex formation between metal compound and functional groups of the forming polymer.[1,2] It is known that segmented polyurethanes are spontaneous nanostructured systems. Analysis of complexation processes occurring in the modified polymer matrix at a molecular level is important to evaluate their influence on macro-characteristics of the polymer system.[3–5]

Influence of method of metal compound introduction in polymer (chemical grafting, polymerization of metal containing monomer, filling etc.) as well as influence of metal ion nature and electron configuration on host polymer structure and properties was analyzed elsewhere.[3–8] To our knowledge, the data related to polymer systems where metal containing modifier includes more then one metal ion in organic environment are absent in literature. Structure-properties relationships of such polymers were not investigated before. In addition, heteropolyionic coordination metal complexes can realize unexpected coordination states of transition metal ions. That, in turn, can give new properties to a polymer formed in their presence.

The objective of this study was to analyze self organization processes and formation of nanostructures in a polymer matrix modified with mono-, bi- and polyheteronuclear complexes of various symmetries as well as to investigate properties of the polymer matrix.

Experimental Part

Materials

Polypropylene glycol M 1000 (PPG) was dried under vacuum at 120 °C for 2 h. Tolylene diisocyanate (mixture 80/20 of 2,4 and 2,6 isomers) (TDI) was distilled under vacuum. Trimethylolpropane (98%) (TMP) was dried under vacuum at 40–45 °C for 2–4 h.

Institute of Macromolecular Chemistry National Academy of Sciences of Ukraine, Kharkov chaussee 48, Kiev 02160, Ukraine
Fax: +(38044) 5524064
E-mail: kozaksmalt@ukr.net

Transition metal β-diketonates - nickel acetylacetonate ($Ni(acac)_2$), chromium acetylacetonate ($Cr(acac)_3$) and cobalt acetylacetonate ($Co(acac)_3$)- were dried under vacuum. Copper ethylacetoacetate ($Cu(eacac)_2$) has been recrystallized.

Polyheteronuclear metal complexes of Cu(2+), Cd(2+), Zn(2+), Ni(2+) and Co(3+), described elsewhere,[9] were provided by Prof. V. Kokozay (Kiev Taras Shevchenko University). The complexes $[Cd_2Cu_2J_4(Me_2Ea)_4(dmso_2)]$, $[Cd_2Cu_3Br_6(Me_2Ea)_4(dmso_2)]$, $[Cu_2Zn(NCS)_3(Me_2Ea)_3]\cdot CH_3CN$, $[Cu_2Zn(NH_3)Br_6(Me_2Ea)_3]$ and $[Cu_2Zn_2(NH_3)_2Br_2(HDea)_4]Br_2$, where Ea –amino ethanol, Me_2Ea – 2- dimethyl amino ethanol and Dea – diethanolamine, were dried under vacuum.

N,N′-Dimethylformamid (DMFA), dichloromethane (CH_2Cl_2) and 1,4-dioxane have been distilled.

Polymerization Procedure

Synthesis of the cross-linked metal containing PU was carried out in two stages.

At the first stage the prepolymer was synthesized by the reaction of PPG and TDI taken in the ratio of 2:1 (Scheme 1, a).

At the second stage the prepolymer was mixed with TMP (cross-linking agent) and metal complex (1–5 wt %) (Scheme 1, b). The transition metal complexes were introduced into reaction mixture as solution ($0{,}5\cdot10^{-4}$ to $5{,}0\cdot10^{-4}$ mol/l) in DMFA, 1,4-dioxane or dichloromethane. Reaction was carried out at 37–60 °C for 2,5–3 h.

The PU networks were postcured for 12–24 h depending on used solvent and metal complex. Solvent traces were withdrawn from PU films under vacuum at room temperature up to achievement of constant weight.

The resulted modified PU films are transparent and homogeneously colored in accordance with the color of modifier used.

Hereinafter we will use the following designation of the PU networks analyzed:

PU-0 – metal free polyurethane**;**
PU-Co, PU–Cr, **PU-Ni** and **PU-Cu** – polyurethanes modified by 1% wt of $Co(acac)_3$, $Cr(acac)_3$, $Ni(acac)_2$ and $Cu(eacac)_2$, correspondingly**;**
PU-Cu_2Cd_2J, PU-Cu_3Cd_2Br, **PU-Cu_2Zn-NCS, PU-Cu_2ZnNH_3** and **PU -$Cu_2Zn_2NH_3$**- polyurethanes modified by complexes $[Cd_2Cu_2J_4(Me_2Ea)_4(dmso_2)]$, $[Cd_2Cu_3Br_6(Me_2Ea)_4(dmso_2)]$, $[Cu_2Zn(NCS)_3(Me_2Ea)_3]\cdot CH_3CN$, $[Cu_2Zn(NH_3)Br_6(Me_2Ea)_3]$ and $[Cu_2Zn_2(NH_3)_2Br_2(HDea)_4]Br_2$, correspondingly**;**
PU–Co5% and **PU–Cr5%** - polyurethanes modified by 5% wt. of $Co(acac)_3$, $Cr(acac)_3$, correspondingly**.**

Techniques

EPR-method

EPR-spectra were recorded at temperature 20 °C using 3-cm radiospectrometer PE-1306 equipped with frequency meter

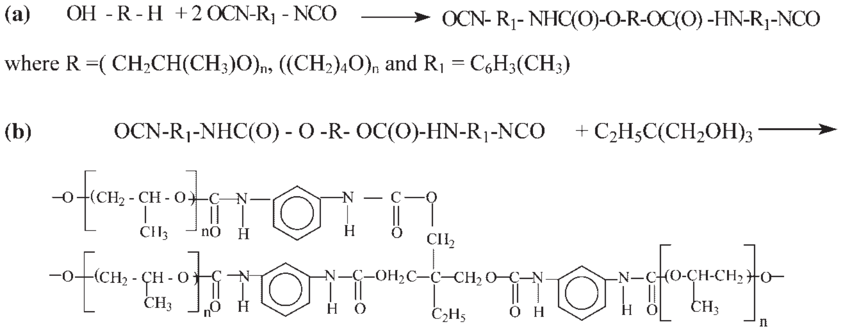

Scheme 1.
Two stage synthesis of PU network.

ChZ-54. The magnetic field was calibrated using 2,2-diphenil-1-pycrilhydrazyl (DPPH) ($g = 2{,}0036$) and ions of $Mn(2+)$ in MgO matrix ($g = 2{,}0015$).

Stable nitroxide radical 2,2,6,6-tetramethylpiperidinyl-1-oxy (TEMPO) was used as paramagnetic spin probe (SP). Nitroxide SP was introduced into PU films via diffusion of its saturated vapor at 30 °C for 2 hours with subsequent keeping at 20 °C for 24 hours.

Correlation time (τ) of SP rotational diffusion in the range of its fast motion ($10^{-11} < \tau < 10^{-9}$ s) was calculated according[10] follows:

$$\tau = 6,65\Delta H_{(+1)}(\sqrt{I_{+1}/I_{-1}} - 1) \times 10^{-10}c, \qquad (1)$$

Where $\Delta H_{(+1)}$ – is width of the central component of TEMPO EPR-spectrum, I_{+1} and I_{-1} - are intensities of low-field and high-field components of the spectrum, correspondingly.

X-ray Scattering Data

Wide-angle X-ray scattering (WAXS) profiles of studied samples were recorded on a Dron-4-07 difractometer with Ni-filtered Cu-K_α radiation and Debay-Sherer optical scheme.[11] Small-scale order parameter (d) was estimated using Bragg's equation: $d = n\lambda/2\sin\theta_m$, where $2\theta_m$ is the position of the diffuse maxima $I(\theta_m)$.

Small-angle X-ray scattering (SAXS) profiles were recorded using KPM-1 X-ray camera.[12] X-ray measurements were carried out using CuKα radiation and monochromatic Ni-filter of CuKα radiation at temperature 22 ± 2 °C with a Schmidt pinhole collimation.[13]

Microscopy

Scanning Electron Microscopy (SEM) has been applied to investigate the morphology of metal containing PU with a JEOL JSM-5400 instrument. SEM micrographs were obtained using 25 kV secondary electrons. The PU samples were frozen under liquid nitrogen and then fractured, mounted, coated with gold/palladium on a Balzers SCD 050 Sputer Coater.

Optical light transmission micro images were obtained by means of microscope MBC-9 with digital video eyepiece ICM532 (magnification of 100) with image processing software AMCAP and VIDCAP.

Differential Scanning Calorimetry (DSC)

Thermal transitions were obtained using differential calorimeter Du Pont 1090 operating in temperature range from −100 to +197 °C. Heating rate was 10° per minute.

Dielectric Relaxation Spectroscopy (DRS)

Two-electrode statistical method of conductivity measurement at a direct current was applied at 10 V.[14]

Complex dielectric permittivity, $\varepsilon^* = \varepsilon' - i\varepsilon''$, of disc-like specimens (diameter: 20 mm) sandwiched between gold-coated brass electrodes was measured over the frequency window from 10^2 to 10^5 Hz in the temperature interval from −40 to140 °C using dielectric spectrometer on the base on alternating current bridge R5083 They have been analyzed from the traditional point of view.[15,16] Additional formalisms such as: complex admittance σ^*, electrical modules M^* and impedances Z', Z'' were used according to formulas.

$$\varepsilon' = C_1/C_o, \mathrm{tg}\delta = \omega \mathrm{R}C_1 \text{ and } \varepsilon'' = \varepsilon' \cdot \mathrm{tg}\delta \qquad (2)$$

$$\sigma^* = \sigma' + \sigma'', \sigma' = \varepsilon\omega'', \sigma'' = \omega\varepsilon', \qquad (3)$$

$$M^* = M' + M'', M' = \varepsilon''/(\varepsilon'^2 + \varepsilon''^2), M'' = \varepsilon'/(\varepsilon'^2 + \varepsilon''^2) \qquad (4)$$

$$Z' = M''/(\omega C_o), Z'' = M'/(\omega C_o) \qquad (5)$$

C_o and C_1 – are instrument and standard capacitor capacities, ω – cyclic frequency.

Results and Discussion

Complexation in Cross-linked PU Modified by Coordination Metal Compound

Introduction of the coordination metal compound in reaction mixture is accompanied with formation of numerous donor-

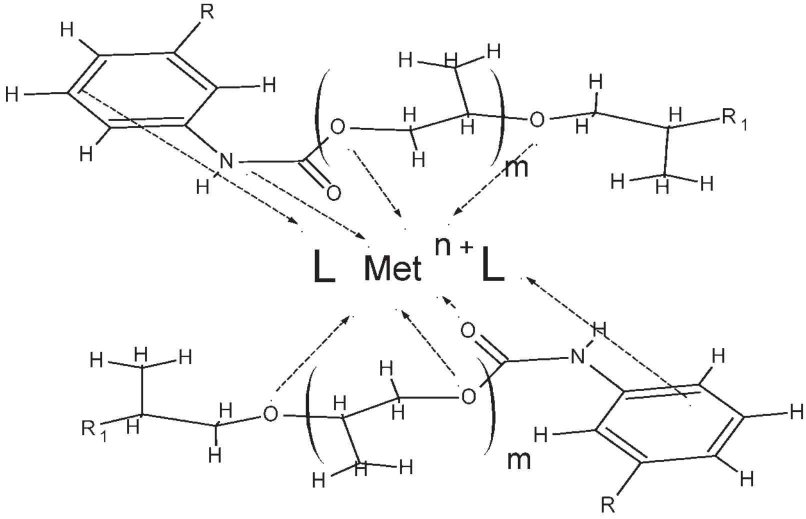

Scheme 2.
Coordination junction point in the modified PU.

acceptor bonds of modifier with the functional groups of forming polymer (Scheme 2). The PU networks modified with transition metal complexes contain both chemical and coordination junctions. Scheme 1, b shows the structure of chemical cross-linkage in a PU network. Scheme 2 shows the possible structure of physical (coordination) junction points of a PU matrix in the presence of metal containing modifiers.

EPR method was used to characterize the state of Cu(2+) ion in copper containing modifiers. This method can give direct information about the state of the paramagnetic ion in generated coordination junction points. Figure 1 illustrates the representative EPR spectra of some copper containing modifiers both isolated and immobilized in PU. Electron-spin parameters calculated from parallel components of EPR spectra are listen in Table 1.

According to experimental and literature data[3–6,17] electron-spin parameters (g-factor and hyperfine splitting constant HFS) as well as EPR spectrum shape are sensitive to symmetry and nature of Cu(2+) neighborhood. In particular, complexing process is accompanied with monotonous increasing of g_{II} in the narrow area 2.29–2.40 and reduction of the HFS constant.[17]

The spectrum of Cu(eacac)$_2$ in frozen glassy solution exhibits narrow components, HFS and anisotropy of g-factor (Fig. 1, a) that indicate the D_{2h} or D_{4h} symmetry of the Cu(eacac)$_2$ chelate node. EPR spectrum of the PU-Cu (Fig. 1, b) also is characteristics for tetragonal copper complexes although with broadened components of the SHF. The calculated parameters of Cu(2+) in PU-Cu differ from the parameters of the unperturbed Cu(eacac)$_2$ (see Table 1). This confirms participation of the modifier in complex formation with the

Table 1.
Electron-spin parameters of isolated and polymer immobilized copper complexes.

System	g||	A|| · 10^4 cm^{-1}	System	g||	A|| · 10^4 cm^{-1}
Cu(eacac)$_2$	2,243	192	[$Cu_2Zn_2(NH_3)_2Br_2(HDea)_4$]$Br_2$	2,370	122
PU-Cu	2,249	150	**PU-Cu$_2$ZnNH$_3$**	2,370	132
				2.300	142

*)Parameters of two complexes that can be approximately resolved in the EPR spectrum of PU-CuZnNH$_3$.

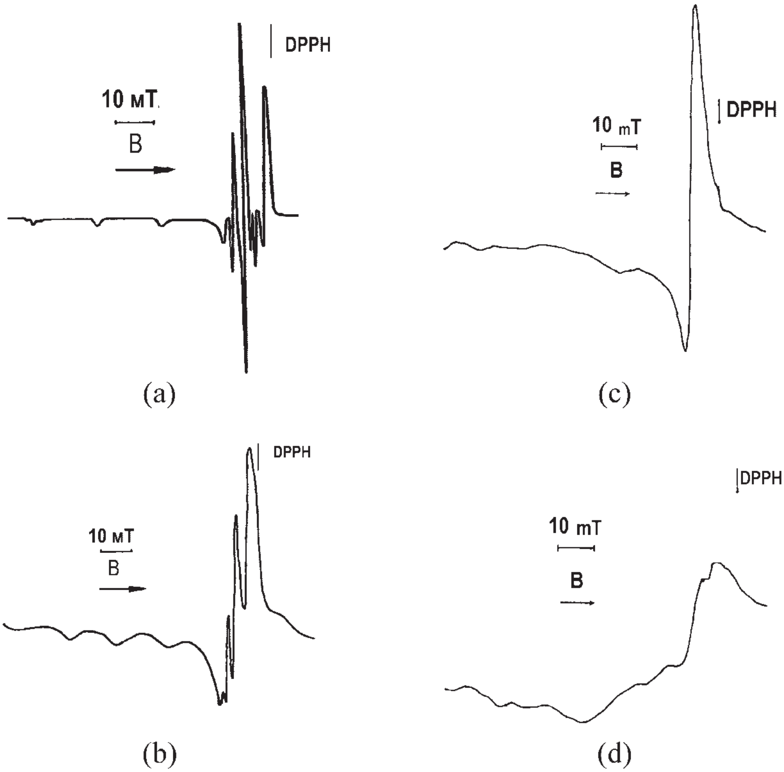

Figure 1.
EPR – spectra of matrix isolated Cu(eacac)$_2$ in chloroform-toluene at −196 °C (a); **PU-Cu** (b); powdered [$Cu_2Zn_2(NH_3)_2Br_2(HDea)_4$]$Br_2$ (c) and **PU-Cu$_2$ZnNH$_3$** (d).

polyurethane network. Comparison of A_{II} and g_{II} values in analyzed PU systems with model systems allows supposing preferred interaction of Cu(eacac)$_2$ with ether oxygen of PU.

The EPR spectra of polyheteronulcear powdered crystalline samples have anisotropic shape with weakly resolved HFS due to broadening of the component (Fig. 1, c) and possible tetrahedral distortion of the copper ion surrounding in the polyionic complex. Immobilization of such complexes in a PU network results in decreasing of the EPR signal intensity (Fig. 1, d). The most reasonable explanation for this effect is distortion of the modifier's symmetry or geometry in PU-CuCd, PU-CuNiCo, and PU-CuZn. The shape of EPR signal in PU network modified with [$Cu_2Zn_2(NH_3)_2$-$Br_2(HDe)_4$]Br_2 indicates formation of complexes of various content and structure.

It should be noted that appearance of HFS in EPR spectra of the modified PUs indicates amorphous character of the solid matrix.

Analyzing polymer system using nitroxide SP (TEMPO in our case) we used the dependence of EPR spectrum of the probe on its rotational and translational mobility in polymer. The last characteristics in turn are determined by structure and mobility of polymer matrix surrounding the probe. In PU matrices that contain Cu^{2+}, Ni^{2+}, Zn^{2+}, Cr^{3+}, Co^{3+}, Cd^{2+} ions EPR spectra of SP are of complex structure and have asymmetric shape (Figure 2, b–c). In all of the spectra occurs essential increasing of central component and broadening of all components in comparison with its spectrum in homogeneous glycerin matrix. The peculiarities observed are most likely the result of signal superposition of fast'' and

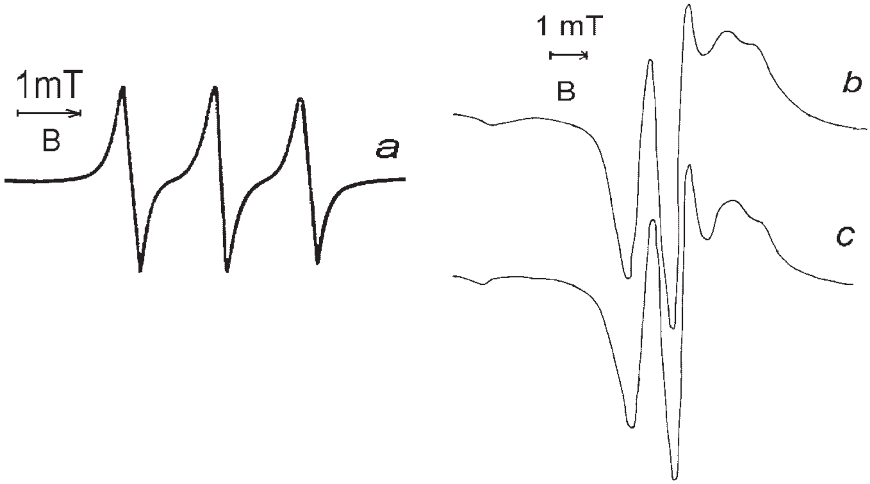

Figure 2.
EPR – spectra of nitroxide SP in glycerin (a), **PU-0** (b) and **PU-Cu** (c).

"slow" probes that are introduced into polymer regions with different mobility.

As it can be seen from the Table 2, tri- and bivalent metal β-diketonates influence rotational mobility of spin probe in the opposite direction:

$$\tau_{PU-Cr} \approx \tau_{PU-Co} > \tau_{PU-0} > \tau_{PU-Cu} > \tau_{PU-Ni}$$

It should be noted that there is no correlation in obtained τ values of polyheteronuclear complexes with exception of most noticeable changes as compared with PU-0.

Morphology of PU Networks Modified by 1% wt of Transition Metal β-Diketonate

Figure 3 shows the WAXS curves and SAXS profiles of metal free PU and PU modified by $Co(acac)_3$, $Cr(acac)_3$, $Ni(acac)_2$ and $Cu(eacac)_2$.

WAXS diagrams of PU-Co and PU-Cr demonstrate two diffuse maxima at $2\theta \approx 19.7^\circ$ (primary) and $2\theta \approx 11.9^\circ$ or $2\theta \approx 12.7^\circ$ (secondary) (marked with arrows in Fig. 3, a). The secondary diffraction maximum is absent on WAXS diagrams of PU modified with bivalent metal β-diketonates. The existence of a main asymmetric diffuse maximum on WAXS- profiles of the PUs with angular position (*2θm*) and small-scale order parameter of 0.44 nm shows that PUs matrices are amorphous. The secondary diffuse maximum is characteristic for the larger average distance between atomic layers in PU matrices as compared with the main maximum (see Table 3).

Modified PUs have microheterogeneous structure typical for segmented polyurethane[19] that are nanostructured systems themselves The intensity maximum on SAXS-profiles of these systems (Figure 3,

Table 2.
Nitroxide SP correlation time.

System	PU-0	PU -Cu	PU -Ni	PU -Cr	PU -Co
$\tau \cdot 10^{10}$ sec	48	42	50	49	43
System	PU -Cr5%	PU -Co5%	PU - CuCd	PU -CuZn	PU - CuNiCo
$\tau \cdot 10^{10}$ sec	50	49	45	32	51

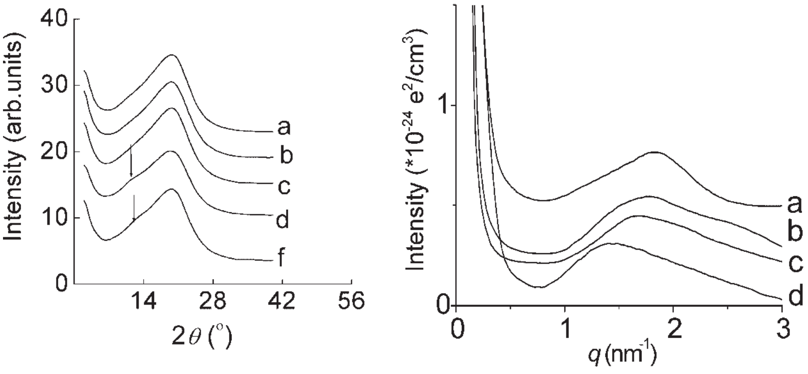

(1) (2)

Figure 3.
X-ray scattering data: WAXS profiles of PUs (1) where **PU-0** (a), **PU-Cu** (b), **PU-Ni** (c), **PU-Cr** (d), **PU-Co** (f) and SAXS profiles of PUs (2) where **PU-Cr** (a), **PU-Co** (b), **PU-0** (c), **PU-Cu** (d).

b) suggests the existence of changeover period of uniform electronic density scattering elements and areas of uniform distribution of hard and flexible blocks of PU chain. Table 4

The position of the scattering intensity maxima as well as the obtained D values of PUs are inverse for tri- and bivalent metal β-diketonate modifiers and can be arranged as follows:

$$D_{\mathrm{PU-Cu}} \approx D_{\mathrm{PU-Ni}} > D_{\mathrm{PU-0}} > D_{\mathrm{PU-Co}} \approx D_{\mathrm{PU-Cr.}}$$

These results correlate with EPR data where a similar arrangement was constructed for mono ionic modifiers.

Morphology of PU Networks Modified by 5% Trivalent Transition Metal β-diketonates

Increasing of metal chelate concentration in PU matrix reveals the phenomenon of saturation of coordination-able sites in the PU matrix. The saturation results in formation of $Co(acac)_3$ and $Cr(acac)_3$ enriched micro-regions in the amorphous PU matrix and segregation of the micro crystals. We can see several groups of discrete diffraction maxima that appear on WAXS diagram of PU-Co5% and PU-Cr5% (Figure 4).

Positions of the discrete diffraction maxima on PU-Co5% and PU-Cr5% WAXS diagrams coincide with the positions of the secondary diffuse maxima on the PU-Co and PU-Cr diagrams, respectively. Taking

Table 3.
WAXS-data for PUs.

System	Characteristics of diffuse maxima				
	The main		The secondary		
	$2\theta_m$	d	$2\theta_m$	d	L
	degree	nm	degree	nm	nm
PU-Cu	19.7	0.44	—	—	—
PU-Ni	19.7	0.44	—	—	—
PU-Cr	19.7	0.44	11.9	0.74	3.7
PU-Co	19.7	0.44	12.7	0.69	3.0

Table 4.
SAXS data for PUs.

System	PU-Cu	PU-Ni	PU-0	PU-Cr	PU-Co
q_m[a] / nm^{-1}	1.48	1.54	1.65	1.90	2.01
D[b] / nm	4.2	4.1	3.8	3.3	3.1

[a] The q value at maximum intensity of $I(q_m)$.

[b] Bragg's period of uniform electronic density scattering elements $D = 2\pi/q_m$, where $q_m = (4\pi/\lambda)\sin\theta_m$.

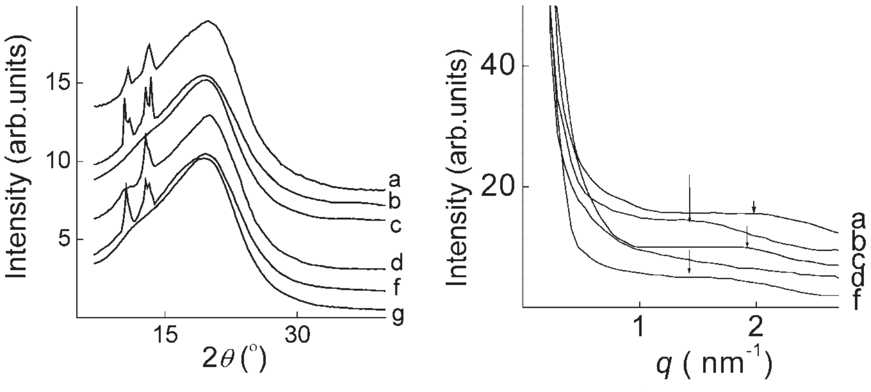

(1) (2)

Figure 4.
X-ray data for PUs modified by 5% trivalent metal β-diketonates: WAXS difractograms (1): **PU-Co5%**(CH_2Cl_2) (a), **PU-Co5%**(DMFA) (b), **PU-Co**(DMFA) (c), **PU-Cr-5%**(CH_2Cl_2) (d), **PU-Cr5%**(DMFA) (f), **PU-Cr**(DMFA) (g). SAXS profiles (2): **PU-Co** (a), **PU-Co5%** (b), **PU-Cr** (c), **PU-Cr5%** (d), **PU-0** (f).

into account that result, we can suppose that even in the presence of small amounts of the trivalent metal β-diketonate in PU there can form micro areas enriched with the modifier (possible nucleation sites). Using WAXS secondary maxima characteristics and Scherrer's formula $L = k\lambda/(\beta cos\theta_m)$[18] dimension of the aggregates could be estimated. Here X-ray wavelength $\lambda = 1.54$ Å, k is the shape factor assigned to 0.9, L is the average diameter of the crystals in angstroms, θ_m is the Bragg's angle in degrees, and β is the half-width of angle diffraction in radians. The value of L is equal to3.0 nm for PU-Co and it is equal 3.7 nm for PU-Cr. It still allow polyurethane matrix to remain amorphous.

The SAXS data that characterize PU-5%Co are similar to characteristics of metal free PU, whereas PU-5%Cr gives SAXS profile without maximum. Presence of 5% wt of trivalent metal complex in the reaction mixture leads to decreasing of the SAXS intensity $I(q_m)$ and shift of q_m to smaller values (Figure 4 part 2) as compared with PU-Co and PU Cr. Segregation of the micro crystals has been also fixed by SEM and transmission optical micro images illustrated on Figure 5.

In addition the SEM images of metal-containing PUs demonstrate the presence in the films of various heterogeneities with 10 to 100 nm linear dimensions as well as heterogeneities with 10 to100 μm linear dimensions. The images reveal both spherical species homogeneously dispersed in amorphous phase and segregation of the crystals (Fig. 5, a–b) in PU-Cr5%. As it can be seen from Figure 5, b such crystals are built of small spherical and ellipsoidal species.

Morphology of PU Networks, Modified by Polyheteronuclear Complexes

PU matrices modified by. polyheteronuclear metal complexes are amorphous. Only one asymmetrical diffusion maximum with $2\theta_m \sim 19{,}5$ is present on WAXS difractograms of the systems (Figure 6). However according to SAXS data microheterogeneity of the PUs changes essentially. Introduction of polyheteronuclear complexes is accompanied by increasing of both the period D and heterogeneity range. In addition we can see significant increase of intensity of scattering in a region from 0.1 up to 0.6 nm (Figure 6 and Table 5).

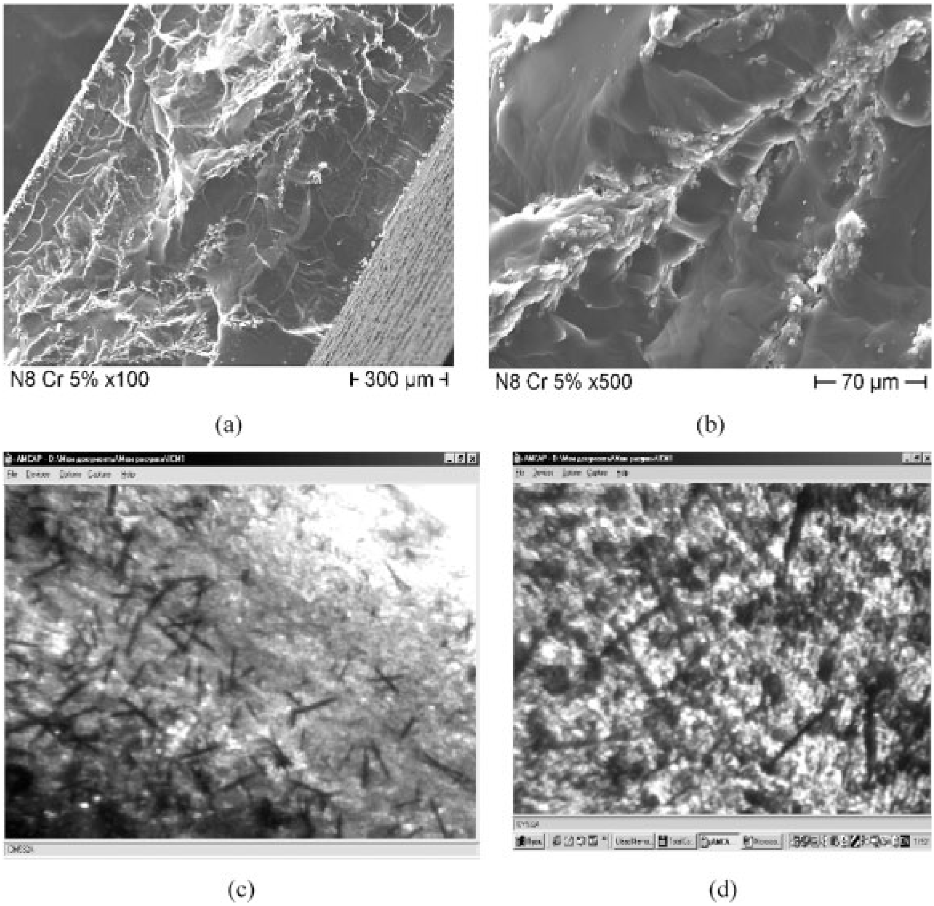

(a) (b) (c) (d)

Figure 5.
SEM-images of cryogenic cross-fractured surface of **PU-Cr5%:** magnification of 100 (a) and magnification of 500 (b); Optical micro images of **PU-Cr5%** (c) and **PU-Co5%** (d).

Microphase separation appears sensitive to polyheteronuclear modifier structure. Maxima on SAXS-profiles were detected for PU-Cu_2ZnBr and PU-$CuNiCoH_2O$ samples whereas SAXS-profiles were detected for PU-Cu_2ZnBr and PU-$CuNiCoH_2O$ samples whereas for PU-Cd_2Cu_3Br and PU -CuNiCoNCS such maxima are absent (Figure 7).

Dielectric Properties

Measurement of direct current conductivity of modified PUs using two-electrode method shows the drastic change of the characteristic (from insulation to semiconductance) depending on metal ion content in modifiers (Table 6). It should be noted that introduction of 1% wt of metal complex into PU is equivalent to introduction of ~0.05% wt of metal ion. That fact and coordination immobilization of the modifiers in polymer makes unlikely increasing of the conductivity level due to the metal compound conductive properties.

Analysis of complex dielectric permittivity as well as complex admittance σ^*, electrical modules M^* and impedances Z', Z'' allows to test character and nature of the conductivity.

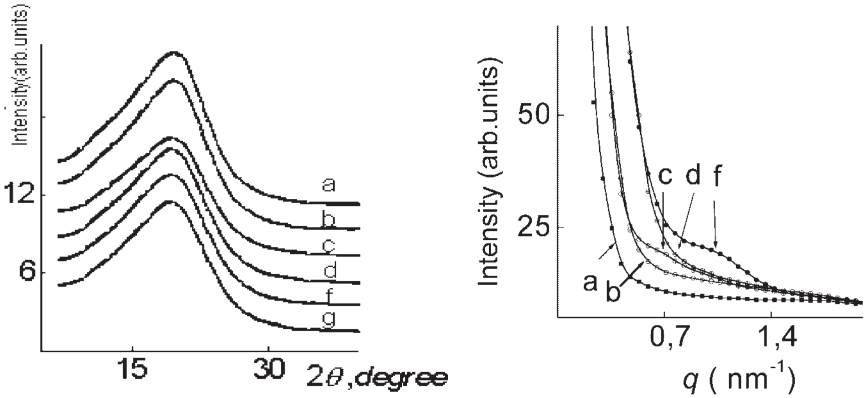

(1) (2)

Figure 6.
WAXS difractograms (1) **PU- 0** (a), **PU-Cu** (b), **PU-Cu3Cd2Br** (c), **PU- Cu$_2$ZnBr** (d), **PU-CuNiCoH$_2$O** (f), **PU-CuNiCoNCS** (g). SAXS profiles (2) of **PU- 0** (a), **PU-CuNiCoNCS** (b), **PU-CuNiCoH$_2$O** (c), **PU-Cd$_2$Cu$_3$Br** (d), **PU-Cu$_2$ZnBr** (f).

Figure 7 illustrates obtained DRS dependences. Calculated conductivity values are listed in the Table 6.

Only conductivity relaxation is obvious in the frequency window of 10^2–10^5 Hz on the frequency and temperature dependences of $\varepsilon''$and M'' for polyheteronulcear modifiers (e.g. PU-Cu$_2$ZnNCS).

On the contrary, two dispersion regions are present on the $\varepsilon''(f)$ and $M''(f)$ dependencies for PU-0 - both the conductivity relaxation and the dipole relaxation. We can made such a conclusion based on the absence of maxima on the $\varepsilon''(f)$ dependencies (Fig. 7, b) and appearance of the maxima on $M''(f)$ dependencies for PU-Cu$_2$ZnNCS (Fig. 7, c). For PU-0 $\varepsilon''(f)$ dependence has at 60 °C non-monotone character (Fig. 7, a). According to[15,16] such behavior is stipulated by two processes: conductivity relaxation in low-frequency range and dipole relaxation in high-frequency range.

Table 5.
SAXS data of PUs.

System	PU-0	PU-Cu	PU-Cu$_2$ZnBr	PU- CuNiCoH$_2$O
q_m / nm^{-1}	1.65	1.48	1.04	0.68
D / nm	3.8	4.2	6.0	9.2

M''(f) dependencies have well defined maxima in temperature region of 20 to 80 °C. According to[16] these maxima correspond to conductivity relaxation. Increasing of temperature is accompanied with shift of conductivity relaxation maxima to higher frequencies (Figure 7-c). Electrical module spectra and $\varepsilon'(f)$ and $\varepsilon''(f)$ dependencies indicate increased mobility of the modified PUs.

Constant σ' values in a high-frequency region corresponds to direct current conductivity σ_{dc}[20] (Figure 7-d). As it can be seen, σ_{dc} grows with increasing of temperature. The effect is characteristic to mechanism of ionic conductivity. The metal ion participation as current carrier is unlikely because to small amounts of metal ion in the modified PUs and immobilization of the modifiers in polymer matrix. A lot of protons presented in PU matrix and observed increasing of polymer chain mobility in modified PUs allows us to suppose proton participation in the process of charge transport.

Calculated at various temperatures values of σ_{dc} are given in the Table 6. The DRS data correlate with two-electrode measurements.

Table 6.
PUs conductivity at a direct current.

System	Solvent	σ_{dc} Sm/cm Temperatures °C		
		20	40	80
PU-0	DMFA	$1.5 \cdot 10^{-12}$		
PU-0	CH_2Cl_2	—	—	4.7×10^{-10}
PU-CuCoNiH$_2$O	DMFA	a)$2.6 \cdot 10^{-9}$ b)$1.6 \cdot 10^{-9}$	—	—
PU-CuCoNiNCS	DMFA	a)$3.3 \cdot 10^{-9}$ b)$1.3 \cdot 10^{-9}$	b)1.4×10^{-8}	—
PU-Cu$_2$ZnNCS	DMFA	$2.5 \cdot 10^{-9}$	b)2.3×10^{-8}	b)5.5×10^{-7}
PU-Cu$_2$ZnNCS	CH_2Cl_2	—	b)7.3×10^{-9}	b)1.5×10^{-7}
PU-Cu$_2$ZnNCS	1,4-dioxane	—	b)3.0×10^{-9}	b)6.6×10^{-8}
PU-Cu$_2$ZnNH$_3$	DMFA	a)$0.6 \cdot 10^{-8}$	—	—
PU-Cu$_2$ZnBr	DMFA	a)$1.8 \cdot 10^{-9}$	—	—
PU-Cd$_2$Cu$_3$Br	DMFA	a)$3.8 \cdot 10^{-10}$	—	—
PU-CuCdI	DMFA	a)$4.0 \cdot 10^{-10}$	—	—

a) σ_{dc} measured using two-electrode method.
b) σ_{dc} measured using complex electric resistance data $\sigma_d = d/(AR_{dc})$ and $Z''(Z')$ isotherms (Cole-Cole diagram).

Experimental dependences of logσ_{dc} vs 1/T are non-Arrenius both for PU-0 and metal containing PUs. It fit the theoretical curves of Fogel–Tamman-Fulcher (FTF) equation $\sigma_{dc} = \sigma_o \exp(-B/(T-T_o))$ (Figure 7, g) indicating influence of the PUs free volume on charge transport. The results obtained give evidence of significant influence of structural organization in the modified PU on conductivity level.

Noticeable change of σ_{dc} for the same metal-modified PU obtained using solvents with different complexing ability gives additional argument for influence of local complexation on processes of charge transfer in modified PUs. In some cases σ_{dc} changes due to solvent replacement are greater than σ_{dc} changes due to metal compound replacement (Table 6, Fig. 7, g).

Presence of additional complexing agent in reaction mixture interferes in the structuring process via parallel competitive complexation with modifier and/or polyurethane. Some of the possible complexes of solvent and modifier are illustrated below:

DSC measurements data are illustrated in Figure 8. They give a number of correlations with experimental results discussed in previous sections.

Decreasing of glass-transition temperature of PUs modified by polyheteronuclear complexes indicates the increasing of polymer chain mobility in the modified PUs and correlate with DRS data. Moreover, the correlation could be found between the value of particular PU d.c. conductivity and corresponding decreasing of T_g. (see Table 6 and Fig. 8, b).

Furthermore, tri- and bivalent metal β-diketonates cause opposite changes of T_g. Glass-transition temperatures of the modified PUs can be arranged as follows (Fig. 8, a):

$$T_{g(\mathrm{PU-Cu})} < T_{g(\mathrm{PU-Ni})} < T_{g(\mathrm{PU-0})} \approx T_{g(\mathrm{PU-Co})} < T_{g(\mathrm{PU-Cr})}$$

These results correlate with EPR and DRS data where a similar arrangement was constructed for the same mono ionic modifiers.

Conclusion

Mono- and polyheteronuclear metal complexes were *in situ* immobilized in polymer system based on cross-linked polyurethane.

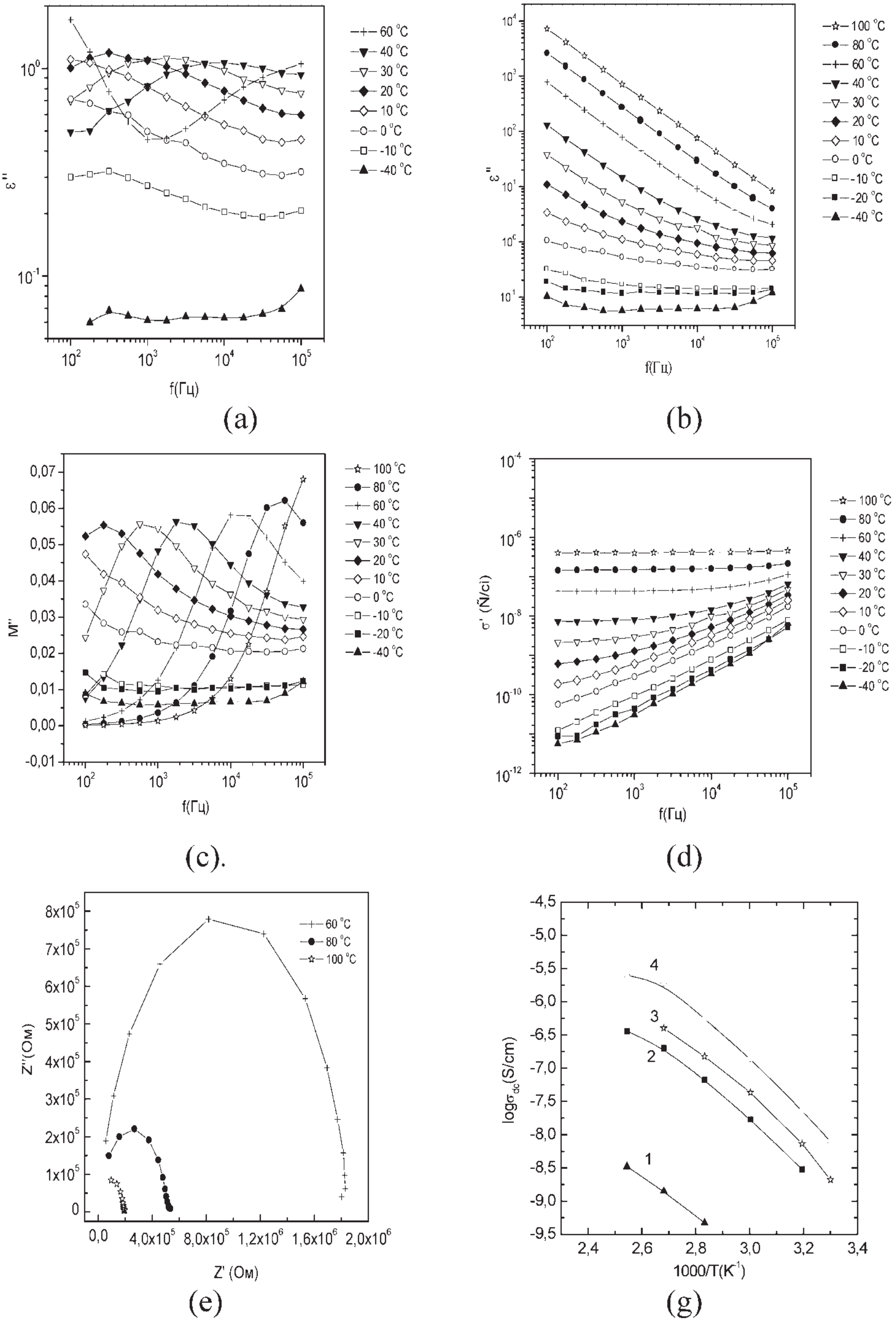

Figure 7.
Representative DRS frequency dependences at various temperatures: ε''(f) **PU-0** (a), ε''(f) for **PU-Cu_2ZnNCS** (b), M''(f) for **PU-Cu_2ZnNCS** (c), σ'(f) for **PU-Cu_2ZnNCS** (d), Z''(Z') for **PU-Cu_2ZnNCS** (e), logσ$_{dc}$ vs 1/T(g) for **PU-0** and **PU-Cu_2ZnNCS** in the presence of 1,4-dioxane (2);dichloromethane(3) DMFA(4).

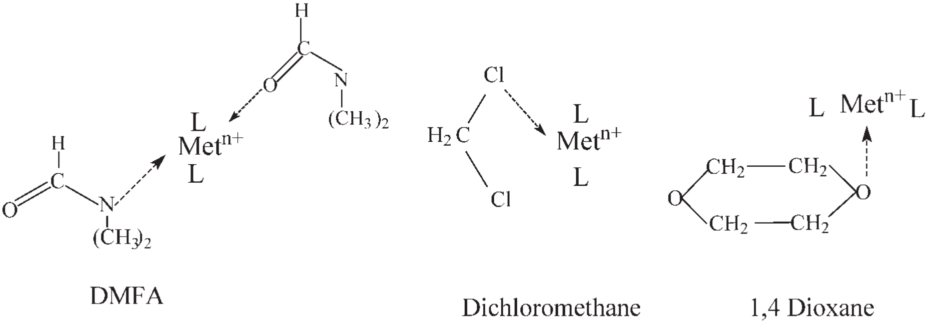

Scheme 3.
Possible coordination of various solvents in the modified PU For PU-Cu_2ZnNCS in the whole temperature region conductivity values can be arranged as follows: $\sigma_{dc}(\mathrm{DMFA}) > \sigma_{dc}(\mathrm{CH_2Cl_2}) > \sigma_{dc}(\text{1,4-dioxane})$.

Obtained systems contain nanoscale structures both organic self-similar microheterogeneities typical for segmented PU and metal-containing coordination junction points. The later contain one or several metal ions in organic environment. Nanoscale dimensions of these aggregates were demonstrated by X-ray data and SEM microscopy. The relationship was found between modified PUs structure and spatial symmetry of coordination sites. The saturation of PU with trivalent metal β-diketonate was detected.

Dielectric relaxation spectroscopy and static two-electrode method demonstrate increasing of some of the PUs ionic conductivity to semi-conducting level. According to DRS, EPR and DSC data the phenomenon observed is caused by the polymer structuring and increasing of macrochain mobility in the presence of modifiers. The supposition can be made about participation of the modified polyurethane protons in charge transfer process.

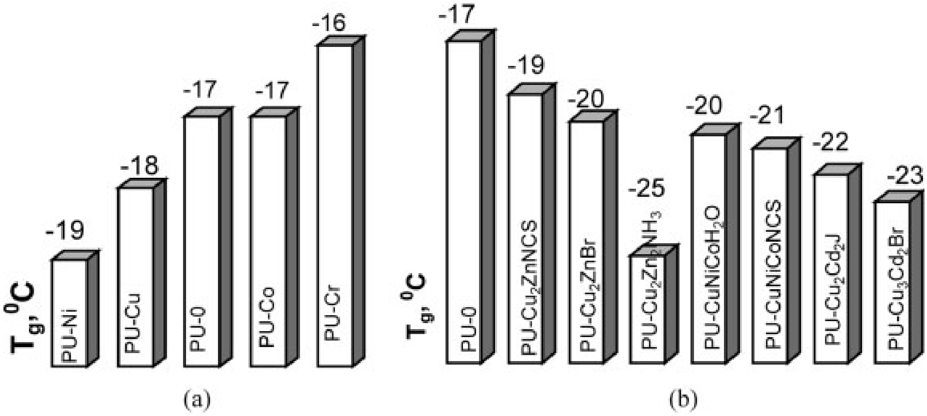

Figure 8.
Glass-transition temperatures of an oligoether component of PUs: modified by metal β-diketonate (a), modified by polyheteronuclear complex (b).

These semi-conductive relatively thermostable (up to 150 °C) and flexible polyurethanes could be of interest as inexpensive high-temperature proton-conducting membranes and as charge dissipative material in electronic devices.

Both synthesis and analysis of structuring in the polymer systems with *in situ* formed nano-scale organic and inorganic microheterogeneities are of interest for design of new *bottom up* nanostructured polymer systems.

[1] J. Ying, in "*Nanostructured Materials: Advances in Chemical Engineering*", Massachusetts Institute of Technology, Cambridge, **2002**.

[2] N.V. Kozak, Yu.M. Nizelskii, V.I. Shtompel, N.V. Mnikh, O.I. Grischuk, *Nanosystems, Nanomaterials, Nanotechnologies* (in Ukrainian) **2005**, 2, 445–464.

[3] Yu.S. Lipatov, L.F. Kosyanchuk, N.V. Kozak et al, *Journal of Polymer Materials* **1997**, *14*, 3, 263.

[4] Yu.S. Lipatov, N.V. Kozak, Yu.N. Nizelskii et al., *Polymer Science. Part A* **1999**, *41*, 8, 1308.

[5] N.V. Kozak, L.F. Kosyanchuk, Yu.N. Nizelskii et al., *Polymer Science. Part A* **2002**, *44*, 7, 1175.

[6] N.V. Kozak, L.F. Kosyanchuk, Yu.S. Lipatov et al., *Theor. and Exper. Chemistry* **2000**, *36*, 2, 90.

[7] L.F. Kosyanchuk, Yu.S. Lipatov, V.F. Babych et al., *Polymer Science. Part A* **2003**, *45*, 7, 1109.

[8] V.A. Vylenskij, V.I. Shtompel, Y.Y. Kercha et al, *Ukr. Chim. J.* (in Russian) **1994**, *10*, 723.

[9] V.N. Kokozay, O.Yu. Vassilyeva, *Transition Metal Chemistry* **2002**, *27*, 693.

[10] A.M. Vasserman, A.L. Kovarskii, "*Spin Labels and Probes in Physical chemistry of Polymers*" (in Russian) Nauka, Moscow, **1986**.

[11] G. Lipson, G. Stipl, "*Interpretation of powder roentgenograms*", Mir, Moscow, **1972**, p. 384.

[12] O. Kratky, I. Pilz, P.J. Schmitz, *J. Colloid Interface Sci.* **1966**, *21*, 1, 24.

[13] P.W. Schmidt, *J. Appl. Cryst.* **1960**, *13*, 480.

[14] V.I. Sazhin in "*Electric properties of polymers*" (in Russian), Khimyia, Leningrad, **1977**, p. 224.

[15] P. Pissis, A. Kanapitsas, *J. Serb. Chem. Soc.* **1996**, *61*, 9, 703.

[16] K. Pathmanatham, G.P. Johari, *J. of Polymer Science: B: Polymer Physic* **1990**, *28*, 675.

[17] A.A. Shkljaev, V.F. Anufrienko, V.D. Ogorodnikov, *J. Struc. Chim. (in Russian)* **1973**, *14*, 6, 994.

[18] A. Ginje in "*X-ray of crystals*", **1961**, p. 392–529.

[19] Yu.S. Lipatov, V.V. Shylov, Y.P. Gomza, N.E. Kruglyak, in "*Research of polymer systems by X-ray method*" (in Russian), Nauk.dumka, Kiev, **1982**.

[20] T. Furukawa, M. Imura, H. Yuruzume, *J. Appl. Phys.* **1997**, *36*, 1119.